11-9-2018

# Redox regulation of type-I inositol trisphosphate receptors in intact mammalian cells.

Suresh K. Joseph
*Thomas Jefferson University*, Suresh.Joseph@jefferson.edu

Michael P. Young
*Thomas Jefferson University*, michael.young@jefferson.edu

Kamil Alzayady
*University of Rochester*

David I. Yule
*University of Rochester*

Mehboob Ali
*Nationwide Children's Hospital*

***See next page for additional authors***

**Authors**
Suresh K. Joseph, Michael P. Young, Kamil Alzayady, David I. Yule, Mehboob Ali, David M. Booth, and György Hajnóczky

# Redox regulation of type-I inositol trisphosphate receptors in intact mammalian cells

Received for publication, August 31, 2018, and in revised form, September 9, 2018 Published, Papers in Press, September 18, 2018, DOI 10.1074/jbc.RA118.005624

**Suresh K. Joseph[‡1], Michael P. Young[‡], Kamil Alzayady[§], David I. Yule[§], Mehboob Ali[¶], David M. Booth[‡], and György Hajnóczky[‡]**

*From the [‡]MitoCare Center, Department of Pathology, Anatomy, and Cell Biology, Thomas Jefferson University, Philadelphia, Pennsylvania 19107, the [§]Department of Pharmacology & Physiology, University of Rochester, Rochester, New York 14642, and the [¶]Center for Perinatal Research, Research Institute, Nationwide Children's Hospital, Columbus, Ohio 43205*

Edited by Ruma Banerjee

**A sensitization of inositol 1,4,5-trisphosphate receptor ($IP_3R$)–mediated $Ca^{2+}$ release is associated with oxidative stress in multiple cell types. These effects are thought to be mediated by alterations in the redox state of critical thiols in the $IP_3R$, but this has not been directly demonstrated in intact cells. Here, we utilized a combination of gel-shift assays with MPEG-maleimides and LC–MS/MS to monitor the redox state of recombinant $IP_3R1$ expressed in HEK293 cells. We found that under basal conditions, ~5 of the 60 cysteines are oxidized in $IP_3R1$. Cell treatment with 50 $\mu$M thimerosal altered gel shifts, indicating oxidation of ~20 cysteines. By contrast, the shifts induced by 0.5 mM $H_2O_2$ or other oxidants were much smaller. Monitoring of biotin–maleimide attachment to $IP_3R1$ by LC–MS/MS with 71% coverage of the receptor sequence revealed modification of two cytosolic (Cys-292 and Cys-1415) and two intraluminal cysteines (Cys-2496 and Cys-2533) under basal conditions. The thimerosal treatment modified an additional eleven cysteines, but only three (Cys-206, Cys-767, and Cys-1459) were consistently oxidized in multiple experiments. $H_2O_2$ also oxidized Cys-206 and additionally oxidized two residues not modified by thimerosal (Cys-214 and Cys-1397). Potentiation of $IP_3R$ channel function by oxidants was measured with cysteine variants transfected into a HEK293 $IP_3R$ triple-knockout cell line, indicating that the functionally relevant redox-sensitive cysteines are predominantly clustered within the N-terminal suppressor domain of $IP_3R$. To our knowledge, this study is the first that has used proteomic methods to assess the redox state of individual thiols in $IP_3R$ in intact cells.**

Inositol 1,4,5-trisphosphate receptor ($IP_3R$)[2] channels serve as the principal mechanism to mobilize $Ca^{2+}$ from endoplasmic reticulum (ER) stores in response to cell stimulation by many hormones, growth factors, and neurotransmitters. The three isoforms of the $IP_3R$ family contain an N-terminal ligand-binding domain, a central regulatory domain, and a C-terminal channel domain. The ligand-binding domain contains a suppressor domain (SD; residues 1–223) that acts to inhibit $IP_3$ binding to the core binding domain (residues 224–604). Channel opening is stimulated when $IP_3$ levels are elevated during agonist stimulation. An alternative mode of channel opening results from regulatory modulation of $IP_3Rs$, which sensitize channels to basal or modest changes in $IP_3$ levels. A well-documented example of $IP_3R$ sensitization results from channel oxidation produced by exogenous or endogenous redox modulators. The first redox agent reported to sensitize $IP_3R$ channels was the organomercurial preservative thimerosal (reviewed in Ref. 1). Other compounds with similar effects include *t*-butylhydroperoxide (2), menadione (3), $H_2O_2$ (4), 2,2′-dithiodipyridine (5), diamide (6, 7), oxidized GSH (8, 9), and superoxide-generating systems such as xanthine/xanthine oxidase (10–13). In the case of thimerosal, the effects on purified reconstituted receptors suggest a direct reaction with thiol groups on the channel (14, 15). The recruitment of multiple $IP_3R$ channels in isolated patches has been shown to be regulated by the redox state of the receptor (16). The effects of prolonged ER stress and enhanced translocation of $Ca^{2+}$ into mitochondria has also been linked to altered $IP_3R$ redox state as a result of hyperoxidation of the ER lumen promoting oxidation of critical intraluminal thiols of the $IP_3R$ (17–19).

Although there is substantial evidence for the regulation of $IP_3Rs$ by redox state, there is very little known regarding which $IP_3R$ thiols are involved, the types of thiol modifications occurring in the intact cell, or how the channel is sensitized by redox modifications. Although changes in $IP_3R$ redox state are presumed to occur, they have never been directly measured. The present study is the first to measure the redox state of $IP_3R$ in intact cells treated with various oxidants and to apply proteomic methods to interrogate the redox state of individual thiols in the $IP_3R1$ isoform, which contains a total of 60 cysteines. These studies identify 4 oxidized thiols under basal conditions and an additional 11 or 4 thiols, which become oxidized in cells exposed to thimerosal or $H_2O_2$, respectively. The functional relevance of these oxidations was investigated using cysteine mutants transfected into a HEK293 $IP_3R$ triple-knockout cell line. The results show that the redox-sensitive cysteines required for $IP_3R1$ channel

This work was supported by National Institutes of Health Grants RO1 DK103558 (to S. K. J. and G. H.) and RO1 DK051526 (to G. H.). The authors declare that they have no conflicts of interest with the contents of this article. The content is solely the responsibility of the authors and does not necessarily represent the official views of the National Institutes of Health.

[1] To whom correspondence should be addressed: Dept. of Pathology & Cell Biology, Rm. 527E JAH, 1020 Locust St., Philadelphia, PA 19107. Tel.: 215-503-1222; E-mail: suresh.joseph@jefferson.edu.

[2] The abbreviations used are: $IP_3R$, inositol 1,4,5-trisphosphate receptor; ER, endoplasmic reticulum; SD, suppressor domain; IAM, iodoacetamide; BSO, buthionine sulfoximine; 3KO, triple-knockout; DB, denaturing buffer.

potentiation are predominantly clustered within the N-terminal suppressor domain.

## Results

We have adapted a method originally described by Leichert and Jakob (20, 21) to measure the redox state of $IP_3Rs$ *in situ* (Fig. 1*A*). The critical initial step is the lysis of cells directly in 10% TCA to prevent any alteration of thiol status. Precipitated proteins are solubilized under strongly denaturing conditions (0.5% SDS, 6 M urea), and free thiols are blocked irreversibly by reaction with 10 mM iodoacetamide (IAM). The samples are then reprecipitated with TCA, and any oxidized thiols are reduced with 10 mM DTT. A further TCA precipitation was used to remove the DTT, and free thiols on the receptor were reacted with PEG-maleimides of different sizes (2, 5, and 20 kDa). The resulting gel shifts can be measured on SDS–PAGE after immunoblotting for $IP_3R$. HEK293 cells were used as an experimental system. These cells contain very low levels of $IP_3R1$ and endogenously express $IP_3R2$ and $IP_3R3$ (22). Data from gel-shift assays are shown in Fig. 1 (*B–E*) for HEK293 cells transfected with $IP_3R1$. Reproducible, small shifts are observed with both MPEG-2 and MPEG-5 under basal conditions (Fig. 1*B*). These shifts are not artifactual because they are blocked by inclusion of DTT during the MPEG reactions (Fig. 1*B*) or by DTT pretreatment of the intact cells prior to lysate preparation (Fig. 1*C*, *lanes 1–3*). The addition of the oxidants $H_2O_2$ (0.5 mM; Fig. 1*C*, *lanes 7–9*) or thimerosal (50 $\mu$M; Fig. 1*C*, *lanes 10–12*) enhanced the shift observed with both MPEG-2 and MPEG-5. Thimerosal produced larger changes than $H_2O_2$, and the effect of both oxidants were not additive (Fig. 1*C*, *lanes 13–15*). There are 60 cysteines in the primary sequence of the rat $IP_3R1$. Lysates prepared in the absence of IAM treatment allow maximum reactivity to be measured, but shifted bands were retained on the gel only for the small MPEG-2 (Fig. 1*D*). In principle, given the molecular weight of the MPEGs, the total number of cysteines involved can be determined from the magnitude of the shift, but quantitation is subject to several inaccuracies and assumptions. One of these is the unusual hydrodynamic properties of MPEG-2 and MPEG-5 that produces gel shifts on SDS–PAGE corresponding to 5 and 15 kDa, respectively (23, 24). Taking this into account, the shifts with either MPEG-2 or MPEG-5 correspond to the presence of ~5 oxidized cysteines/$IP_3R1$ subunit under basal conditions and ~10 and ~20 oxidized cysteines/subunit in the presence of $H_2O_2$ and thimerosal, respectively (Fig. 1*E*). Previous studies have suggested that $IP_3Rs$ in hepatocytes are stimulated by GSSG (25), and $IP_3Rs$ are reported to be glutathionylated in response to diamide in endothelial cells (6, 7). Changes in the GSH redox status of HEK293 cells in response to $H_2O_2$ and thimerosal are shown in Fig. 2*A*. Both thimerosal and $H_2O_2$ caused similar increases in GSSG levels, but only thimerosal caused a large drop in total glutathione (GSH + GSSG). In contrast to $H_2O_2$, thimerosal forms an ethyl mercury adduct with reduced thiols and is known to deplete GSH in other systems (26). Preincubation of cells with buthionine sulfoximine (BSO, an inhibitor of GSH biosynthesis) reduced total GSH and GSSG levels but did not alter basal, $H_2O_2$, or thimerosal-induced gel shifts in $IP_3R$ (Fig. 2*B*). Diamide selectively oxidizes GSH to GSSG (27). An $IP_3R$ gel shift was observed at concentrations of diamide (50 $\mu$M) that did not produce detectable elevations of GSSG (Fig. 2*C*). Higher diamide concentrations (250 $\mu$M), which caused large elevations of GSSG, only produced a small additional gel shift (Fig. 2*C*). Diamide and other oxidants such as menadione and *t*-butylhydroperoxide were no more effective than $H_2O_2$ (not shown). Overall, the data do not show a clear correlation of $IP_3R$ oxidation with the GSH redox state. Rapid reversibility of both the total GSH levels (Fig. 2*D*) and the gel shifts were observed when DTT was added to the cells after the thimerosal (Fig. 2*E*).

To get a comprehensive picture of the status of individual $IP_3R$ cysteines, we adopted a proteomic approach in which the denatured cell lysates prepared after sequential iodoacetamide and DTT treatment were incubated with biotin–maleimide instead of PEG-maleimide (Fig. 1*A*). The modified $IP_3R1$ was then immunoprecipitated from the lysate, separated on SDS–PAGE, and silver-stained. The excised band was subjected to in-gel digestion with trypsin and processed for LC–MS/MS. The mass spectra were interrogated for cysteine containing peptides that were either modified with iodoacetamide (corresponding to reduced thiols) or modified with biotin–maleimide (corresponding to oxidized thiols). The compiled results from three independent experiments derived from control and thimerosal-treated cells are shown in Fig. 3 and Table 1. The mean sequence coverage was 71 ± 2% and resulted in the detection of 41 of 60 total cysteines when trypsin was used for cleavage. We observed four cysteines that were oxidized under basal conditions: Cys-292, Cys-1415, Cys-2496, and Cys-2533. Two of these cysteines are cytosol-facing (Cys-292 and Cys-1415), and two are intraluminal (Cys-2496 and Cys-2533). Thus of the five intraluminal cysteines, only two were oxidized. In the presence of thimerosal, the cysteines oxidized under basal conditions remained oxidized, and an additional 11 cytosol-facing cysteines were identified as being oxidized. These were Cys-37, Cys-206, Cys-638, Cys-767, Cys-897, Cys-995, Cys-1298, Cys-1459, Cys-1522, Cys-1647, and Cys-1976. It should be noted, however, that only six of these cysteines were consistently oxidized in all three trials (*boxed* in Fig. 3 and underlined in Table 1). In the case of Cys-206 and Cys-2533, we were able to identify only the oxidized form of the peptides in the spectra from thimerosal-treated cells. However, with the other redox-sensitive cysteines, both the oxidized and reduced forms of the peptides were evident (Table 1). For several cysteines the observed oxidation events were rare and in some cases observed only once in the three trials. However, the frequency of oxidation events was much higher (35–100%) for the six cysteines that were reproducibly oxidized. Lysates from $H_2O_2$-treated cells were analyzed in two experiments (Fig. 3, *yellow boxes*, and Table 1). A total of six cysteines were oxidized in both trials with three residues found under basal conditions (Cys-1415, Cys-2496, and Cys-2533), and an additional three residues oxidized upon $H_2O_2$ addition (Cys-206, Cys-214, and Cys-1397). The residues repeatedly oxidized by thimerosal and $H_2O_2$ were conserved in all three $IP_3R$ isoforms, with the exception of the thimerosal-sensitive residue Cys-1459, which was present only in the $IP_3R1$ isoform (Fig. 3).

To use a mutagenesis approach to assess the functional role of individual cysteines in redox-modulation of the $IP_3R$ chan-

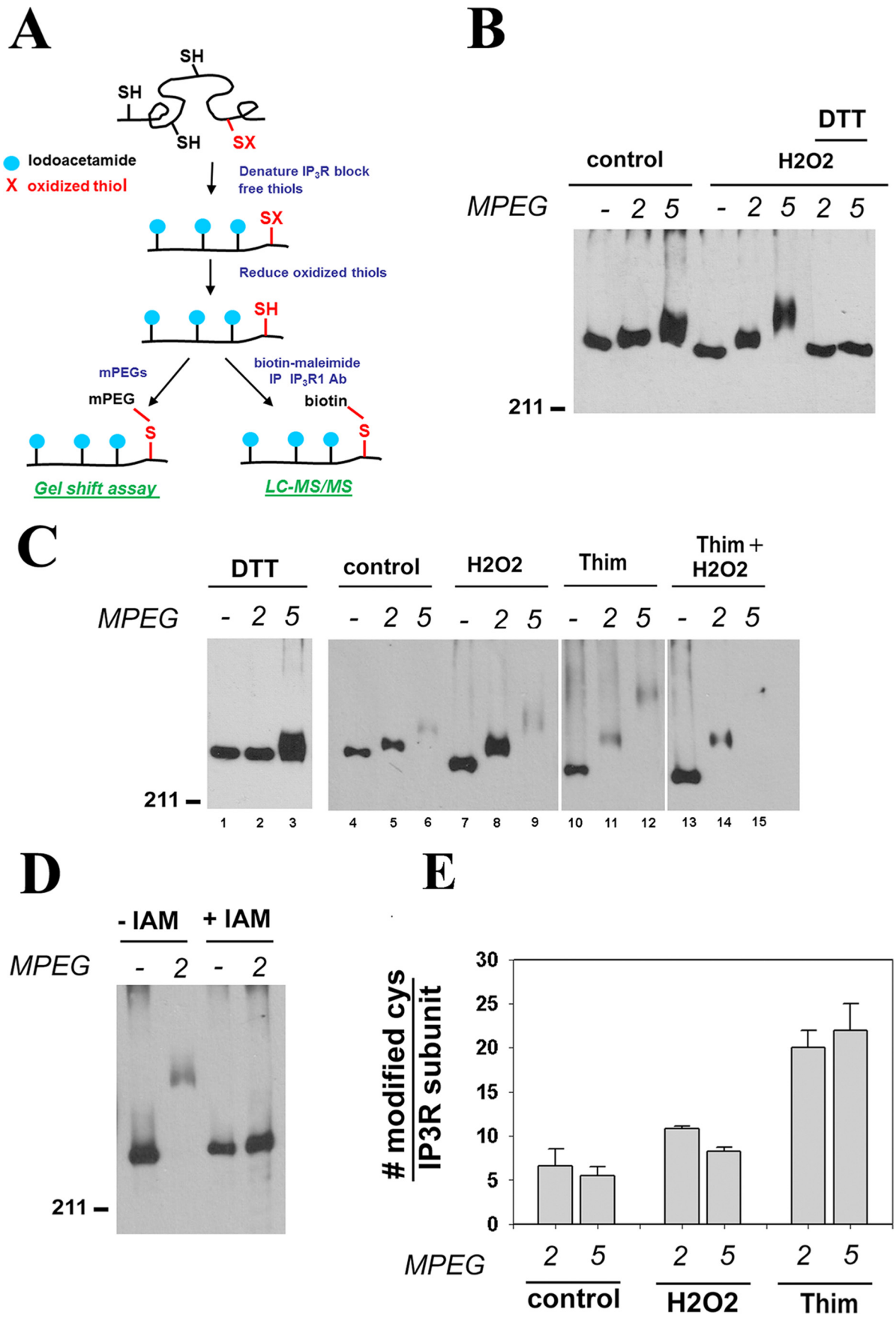

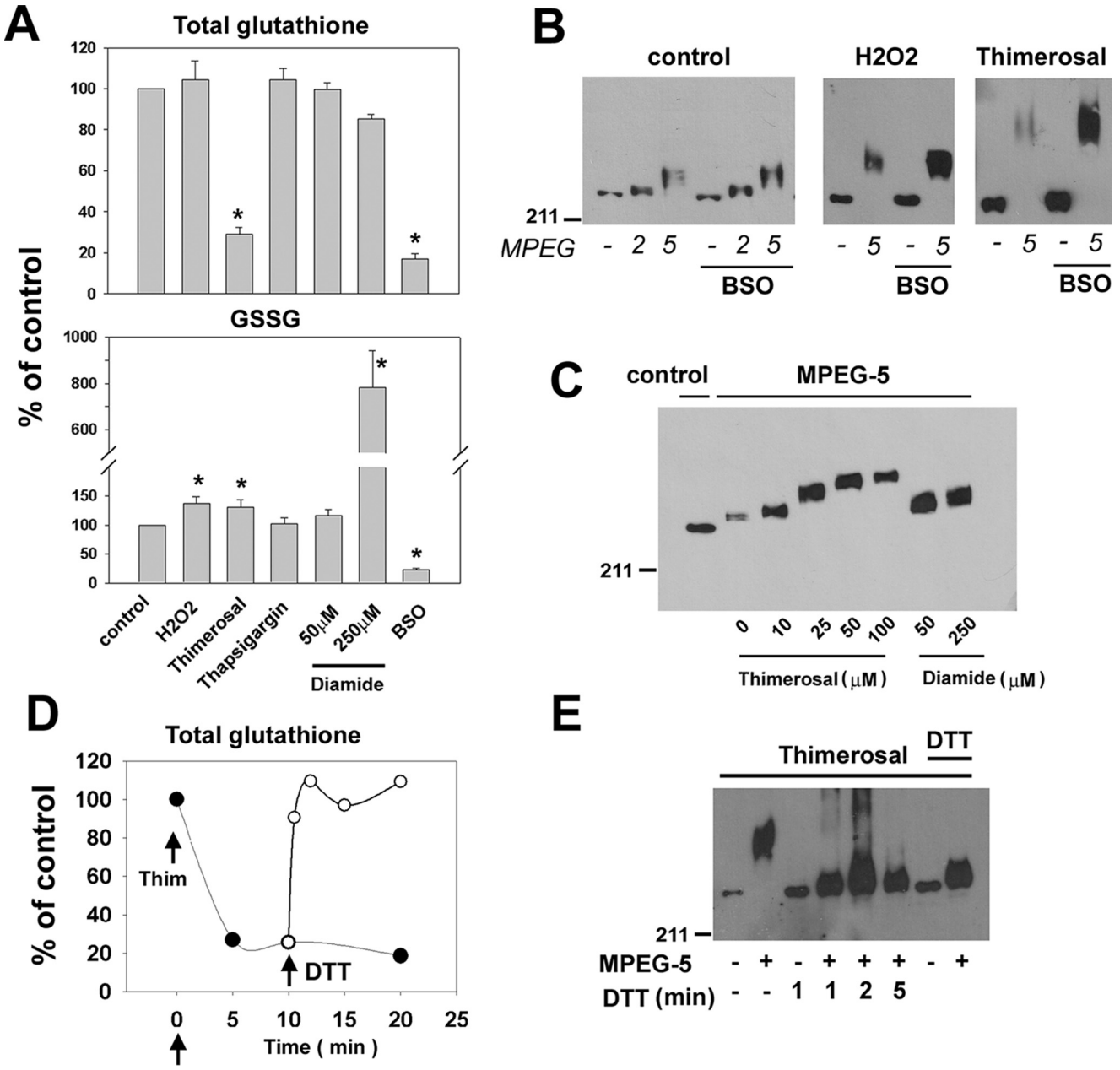


**Figure 2. Additional characterization of $IP_3R$ redox responses.** *A*, total GSH and oxidized GSH was measured after treatment for 10 min with $H_2O_2$ (0.5 mM), thimerosal (50 $\mu$M), thapsigargin (1 $\mu$M), the indicated concentrations of diamide, and 16 h preincubation with 0.25 mM BSO. *B*, gel shift assays after BSO treatment. *C*, gel-shift dose responses for thimerosal and diamide. *D* and *E*, rapid DTT (10 mM) reversibility of thimerosal-induced changes in total GSH (*D*) and $IP_3R$ (*E*) gel shifts. In the *last two lanes*, the DTT was added before the thimerosal.

nel, we chose to employ a recently created human HEK293 cell line from which all three $IP_3R$ isoforms have been deleted by CRISPR (28). These 3KO cells do not elicit agonist or $IP_3$-mediated cytosolic $Ca^{2+}$ signals (28, 29) as illustrated in Fig. 4*A* for stimulation with carbachol in the presence of extracellular $Ca^{2+}$. By contrast, robust carbachol responses are observed in WT cells, and $Ca^{2+}$ signals can be restored in 3KO cells by transfection with $IP_3R1$ DNA (Fig. 4*B*). Comparable gel shifts in response to thimerosal (50 $\mu$M) were observed in $IP_3R1$ transfected WT or 3KO cells (not shown). To assay for redox potentiation of $IP_3R1$, we pretreated the cells for 2 min with thimerosal. In initial trials, we observed that the use of concentrations of thimerosal of >20 $\mu$M induced by itself a delayed increase of cytosolic $Ca^{2+}$ (Fig. 4*C*). This presumably reflects sensitization

**Figure 1. Gel-shift assays to measure $IP_3R$ redox state.** *A*, cartoon showing the sequential treatments employed in the two main assays used in this study. *B* and *C*, TCA precipitates solubilized from HEK293 cells transfected with $IP_3R1$ were sequentially treated with IAM and DTT and then reacted for 1 h with 0.5 mM MPEG-2 or MPEG-5. Gel shifts in $IP_3R$ were assessed by immunoblotting. Treatment of cells was for 10 min with $H_2O_2$ (0.5 mM) and thimerosal (*Thim*, 50 $\mu$M). In *B*, DTT (10 mM) was added during the MPEG reaction, and in *C* (*lanes 1–3*), the cells were pretreated for 30 min with DTT before lysis. *Lanes 4–15* are from the same blot, but a higher exposure of *lanes 10–12* is shown for better visualization of the bands. *D*, IAM (10 mM) treatment of the lysates was omitted as a control. *E*, the number of reactive cysteines was calculated from the magnitude of the gel shift relative to molecular weight markers as described under "Materials and methods." The data shown are the means ± S.E. for three to five measurements. For additional details see text.

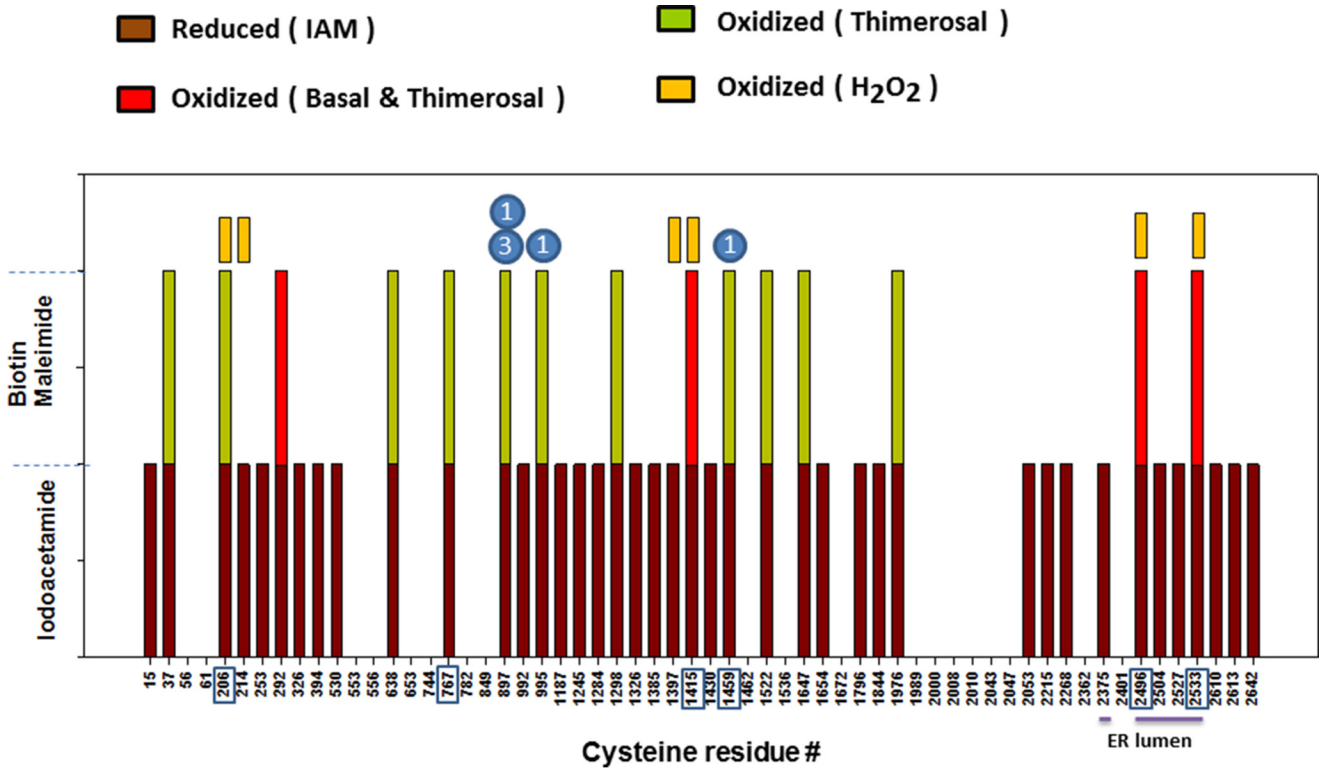


**Figure 3. Identification of redox-sensitive thiols in $IP_3R1$ using LC–MS/MS.** Redox lysates were prepared from transfected HEK293 cells treated in the presence and absence of thimerosal (50 $\mu$M) and processed with IAM to block free thiols. Oxidized residues were liberated with DTT, and the lysate was TCA-precipitated again and reacted with biotin–maleimide (0.5 mM, 5 h). The lysates were processed on a Sephadex G25 column to exchange the sample into a buffer suitable for immunoprecipitation, which was carried out with a C-terminal Ab. The immunoprecipitates were processed on 5% SDS–PAGE, and the silver-stained $IP_3R$ was excised and processed for LC–MS/MS. The spectra were analyzed with the SEQUEST search engine for tryptic peptides containing cysteines modified with IAM (reduced) or biotin–maleimide (oxidized). The *boxed* residues were identified in each of three independent trials. Oxidized residues observed in $H_2O_2$ (0.5 mM)–treated cells are indicated by *yellow rectangles*. Cysteine residues located in the ER lumen are *underlined*. All oxidized residues are conserved in all three isoforms with the exceptions shown in *filled blue circles*.

of $IP_3R1$ to endogenous $IP_3$ because the response to thimerosal was greatly blunted in untransfected 3KO cells (Fig. 4*D*). To be able to measure redox potentiation of carbachol responses, we chose to use a low concentration of thimerosal (10 $\mu$M), which allowed a stable baseline to be maintained during thimerosal pretreatment prior to stimulation by carbachol. The carbachol addition was combined with EGTA to chelate extracellular $Ca^{2+}$ and ensured that only intracellular $Ca^{2+}$mobilization was being measured. Under these conditions a thimerosal-induced potentiation of the $Ca^{2+}$ signal was observed for WT $IP_3R1$ at low subsaturating concentrations of carbachol (Fig. 4*E*) but not at a maximal dose of carbachol (Fig. 4*F*). $IP_3R1$ in which the N-terminal 12 cysteines have been mutated to alanine (Cys-less) has been shown to be a functional channel that is insensitive to a stimulatory effect of thimerosal on [$^3$H]$IP_3$ binding (30, 31). In agreement with these studies, the Cys-less mutant failed to show thimerosal-induced potentiation of $IP_3R$ function in 3KO cells (Fig. 4, *G* and *H*). Thimerosal at higher concentrations has been found to inhibit $IP_3$-mediated $Ca^{2+}$ release (32). It should be noted that in our studies, using 10–50 $\mu$M thimerosal, only stimulatory effects were observed.

A selected group of cysteine mutants were further analyzed for redox potentiation. These mutants included the individual residues within the N-terminal Cys-less construct, as well as three residues that were reproducibly oxidized in the MS assays (C767S, C1415S, and C1459S), and a cysteine found only in the SI(+) alternatively spliced form of $IP_3R1$ (C326S). Several of these mutants have been used in our previous studies (33). The expression of new mutants in 3KO cells was verified by Western blotting (Fig. 5*A*). To quantitate potentiation we measured the ratio of $Ca^{2+}$ responses in the presence and absence of thimerosal pretreatment using 0.25 $\mu$M carbachol as in Fig. 4*C*. The maximal response to 20 $\mu$M carbachol was also measured and normalized to the maximal response observed with WT $IP_3R1$ DNA. The potentiation ratio and maximal responses for each of the mutants are shown in Fig. 5 (*B* and *C*), respectively. Five of the eleven mutants showed diminished potentiation by thimerosal. Of these, four showed a partial inhibition (C37S, C56S/C61S, C214S, and C326S), whereas C15S was almost as effective as the Cys-less in removing the potentiating effect of thimerosal. The majority of the mutants showed maximal carbachol responses that were comparable with the WT $IP_3R1$, although several had significantly lower (*e.g.* C37S) or higher (*e.g.* C15S) responses (Fig. 5*C*). The variation in maximal responses may reflect different levels of functional receptors in the ER stores that may not be evident at the level of immunoblots. It should be noted, however, that the maximal responses did not correlate with diminished redox potentiation.

The residues having no effects (colored *orange* in Fig. 5) include Cys-767, Cys-1415, and Cys-1459, which were all residues that were reproducibly oxidized in MS assays after thimerosal treatment, with Cys-1459 being constitutively oxidized

**Table 1**

**The cysteine residues oxidized by thimerosal in three independent trials are shown in green**

The numbers of occurrences of biotin maleimide-modified peptides (oxidized), carbidomethylated peptides (reduced), or unmodified peptides in these samples are tabulated with the number of experiments shown in parentheses. The underlined residues are where at least one occurrence of oxidized peptide was observed in all three trials. In three trials the cysteine residues that were oxidized under basal conditions were Cys-292, Cys-1415, Cys-2496, and Cys-2533. The numbers of occurrences of peptides containing these oxidized residues were 10 (2), 16 (3), 18 (3), and 6 (3) with the number of experiments shown in parentheses. The oxidized peptides in $H_2O_2$-treated cells were also tabulated for two independent trials.

| Cys residue | #occurrences of oxidized peptide (thimerosal) | #occurrences of reduced peptide (thimerosal) | #occurrences of unmodified peptide (thimerosal) | #occurrences of oxidized peptide ($H_2O_2$) |
|---|---|---|---|---|
| 15 | 0 | 15 (2) | 2 (1) | 0 |
| 37 | 1 (1) | 24 (3) | 0 | 0 |
| 206 | 3 (3) | 0 | 0 | 7 (2) |
| 214 | 0 | 9 (2) | 0 | 6 (2) |
| 253 | 0 | 42 (3) | 0 | 0 |
| 292 | 1 (1) | 13 | 0 | 0 |
| 326 | 0 | 66 (3) | 0 | 0 |
| 394 | 0 | 49 (3) | 2 (1) | 0 |
| 530 | 0 | 137 (3) | 0 | 0 |
| 638 | 3 (2) | 16 (3) | 0 | 0 |
| 767 | 15 (3) | 18 (3) | 0 | 0 |
| 897 | 1 (1) | 7 (3) | 0 | 0 |
| 992 | 0 | 41 (2) | 2 (1) | 0 |
| 995 | 1 (1) | 9 (2) | 0 | 0 |
| 1187 | 0 | 122 (3) | 0 | 0 |
| 1245 | 0 | 55 (3) | 0 | 0 |
| 1284 | 0 | 35 (3) | 0 | 0 |
| 1298 | 3 (2) | 16 (2) | 0 | 0 |
| 1326 | 0 | 53 (3) | 0 | 0 |
| 1385 | 0 | 62 (3) | 0 | 0 |
| 1397 | 0 | 69 (2) | 0 | 2 (1) |
| 1415 | 5 (3) | 9 (2) | 0 | 3 (2) |
| 1430 | 0 | 42 (3) | 0 | 0 |
| 1459 | 5 (3) | 14 (3) | 0 | 0 |
| 1522 | 1 (1) | 8 (3) | 0 | 0 |
| 1647 | 1 (1) | 3 (2) | 0 | 0 |
| 1654 | 0 | 37 (3) | 0 | 0 |
| 1796 | 0 | 141 (3) | 0 | 0 |
| 1844 | 0 | 24 (2) | 0 | 0 |
| 1976 | 2 (1) | 24 (3) | 0 | 0 |
| 2053 | 0 | 6 (1) | 0 | 0 |
| 2215 | 0 | 121 (3) | 0 | 0 |
| 2268 | 0 | 17 (3) | 1 (1) | 0 |
| 2375 | 0 | 21 (3) | 0 | 0 |
| 2496 | 6 (3) | 4 (2) | 0 | 14(2) |
| 2504 | 0 | 12 (2) | 0 | 0 |
| 2527 | 0 | 3 (2) | 1 (1) | 0 |
| 2533 | 6 (3) | 0 | 0 | 3 (2) |
| 2610 | 0 | 10 (3) | 0 | 0 |
| 2613 | 0 | 3 (2) | 0 | 0 |
| 2642 | 0 | 6 (2) | 0 | 0 |

even under basal conditions (Fig. 3). Three residues that are included in the Cys-less mutant but did not appear in the mass spectra (Cys-530, Cys-553, and Cys-556) were also without effect on redox potentiation. The location of the redox-sensitive and -insensitive residues, color-coded as in Fig. 5*B*, have been mapped to the cryo-EM structure of $IP_3R1$ (34) in Fig. 5*D*. The main conclusion is that the redox-sensitive residues are clustered within the first 225 residues. This region has variously been referred to as the suppressor domain (or $\beta$-trefoil domain-1) and has been shown to be critical for channel gating (35–37). The structural implications of these findings are discussed in more detail below.

In the final series of experiments, we have examined the potentiating effects of $H_2O_2$ and also tested the redox sensitivity of the $IP_3R2$ and $IP_3R3$ isoforms (Fig. 6). A maximal dose of carbachol (25 $\mu$M) elicited similar $Ca^{2+}$ responses from $IP_3R1$ and $IP_3R2$ transfected cells and a 20% smaller response in $IP_3R3$ transfected cells (Fig. 6*A*). The dose response to carbachol was examined for all three isoforms (Fig. 6*B*). The $EC_{50}$ for carbachol for $IP_3R1$ (0.62 $\pm$ 0.05 $\mu$M) and $IP_3R2$ (0.66 $\pm$ 0.07 $\mu$M) were similar, although $IP_3R3$ (1.7 $\pm$ 0.12 $\mu$M) was somewhat less sensitive. This can be compared with the rank order of sensitivity $IP_3R2 > IP_3R1 > IP_3R3$ found in direct measurements with $IP_3$ in permeabilized DT40 3KO cells stably expressing different receptor isoforms (13, 38, 39). All of the cysteine mutants also showed similar $IP_3$ sensitivities as the WT $IP_3R1$ (not shown). This is illustrated for the C15S mutant ($EC_{50}$ = 0.76 $\pm$ 0.02 $\mu$M) in Fig. 6*B*. An N-terminal fusion protein containing the Cys-less mutant has also been shown to have a comparable $IP_3$-binding affinity as WT receptors (30). Thus the pronounced loss of redox potentiation seen with the C15S and Cys-less mutants (Fig. 5*B*) is unlikely to be related to an intrinsically different $IP_3$ sensitivity of the channel.

Thimerosal potentiated the carbachol response approximately equally with $IP_3R1$ and $IP_3R2$ isoforms but was much less effective with $IP_3R3$ (Fig. 6*C*). A similar isoform preference was observed when $H_2O_2$ (100 $\mu$M) was used to potentiate carbachol responses. The lack of redox sensitivity of the $IP_3R3$ isoform is in agreement with previous findings in DT40 cells (13, 31). As observed with thimerosal, the C15S $IP_3R1$ mutant was insensitive to potentiation by $H_2O_2$.

## Discussion

Although $IP_3Rs$ have been established to be redox-sensitive channels, the present study is the first to directly measure changes in the redox state of the $IP_3R$ protein in intact cells. To do this, we have utilized gel-shift assays and MS. Although the gel-shift assay is convenient and provides qualitative information, the method is also insensitive, because heterogeneous small shifts in a large protein such as $IP_3Rs$ can be easily missed. Many membrane proteins are known to retain folded structures even in the presence of SDS and urea (40–42). It is therefore possible that not all thiols are freely accessible to the MPEG gel-shift reagent even in the "denaturing" conditions used in our experiments. The MS approach is more sensitive and provides more information. However, this method is limited by incomplete sequence coverage, which resulted in 19 cysteines not being observed in the mass spectrum when the sample was digested with trypsin. Interestingly, the same cysteines were missing in each attempt, including Cys-556 and a cluster of six cysteines located prior to the first transmembrane domain (Fig. 3). To increase coverage, a single trial was conducted with chymotrypsin as the cleavage enzyme, but the same cysteines were also absent in this analysis (not shown). Several recent studies have shown that both ryanodine receptors (43) and $IP_3Rs$ (44) are subject to *S*-palmitoylation. The attachment of palmitic acid is known to interfere with the chromatography of trypsin peptides, making it difficult to identify modified residues by LC–MS/MS (45). Using MALDI–TOF, Cys-56 and Cys-849 were identified as sites of *S*-palmitoylation (44), providing a possible explanation for why peptides containing these sites were absent from the LC–MS/MS analysis. Overall, the limitations in coverage make it likely that the number of redox-sensitive thiols identified by MS is underestimated.

The redox state of the ER lumen is considerably more oxidized than the cytosol, based on the GSH redox couple (46). Therefore, it may be anticipated that the intraluminal thiols of

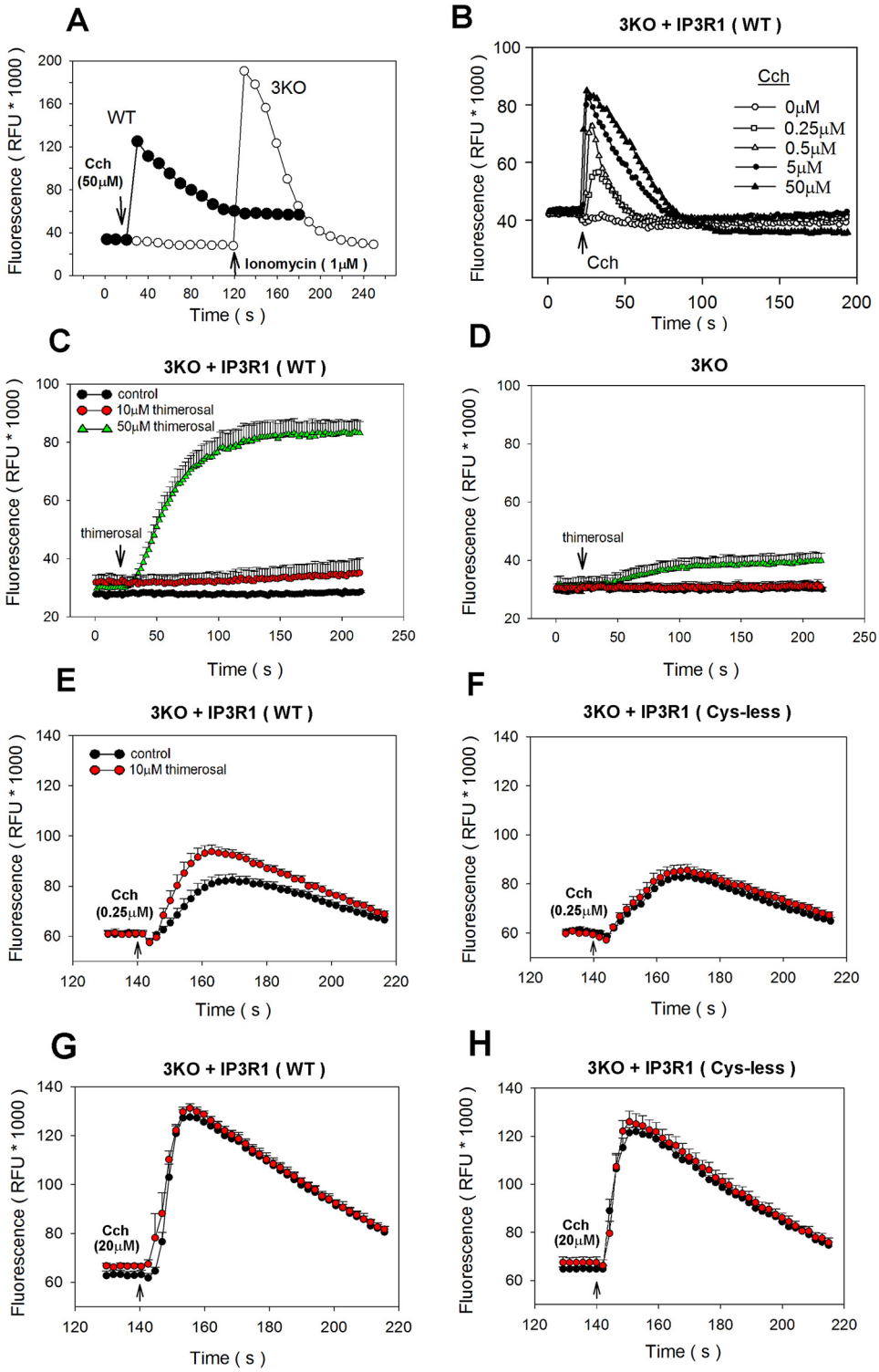


**Figure 4. Measurements of carbachol-mediated cytosolic [$Ca^{2+}$] in HEK293 $IP_3R$ 3KO cells transfected with $IP_3R1$.** Cytosolic free [$Ca^{2+}$] changes were measured with Fluo-8 in 96-well plates on a Flex station apparatus as described under "Materials and methods." *A*, representative traces showing responses of WT and $IP_3R$ 3KO HEK293 cells to a maximal dose of carbachol (*Cch*) in the presence of extracellular $Ca^{2+}$. *B*, changes in cytosolic $Ca^{2+}$ of 3KO cells transfected with $IP_3R1$ and stimulated with the indicated concentrations of carbachol. EGTA (1.3 mM) was added together with the carbachol to chelate extracellular $Ca^{2+}$. *C*, thimerosal (10 or 50 $\mu$M) was added at 18 s to 3KO cells transfected with $IP_3R1$. Cytosolic $Ca^{2+}$ changes are shown as the means ± S.D. of Fluo-8 fluorescence for four wells of a representative experiment. *D*, as in *C* but using untransfected 3KO cells. *E* and *G*, 3KO cells transfected with $IP_3R1$ were stimulated with a submaximal (*E*) or maximal dose (*G*) of carbachol in the absence of extracellular $Ca^{2+}$ under control conditions (*black symbols*) or after pretreatment with 10 $\mu$M thimerosal (*red symbols*) for 2 min. *F* and *H*, as in *E* and *G* but with 3KO cells transfected with a cysteine-less $IP_3R1$ construct in which the first 12 N-terminal cysteines are mutated to alanine (31). The data shown for *E–H* are the mean ± S.D. of four wells from a representative experiment. Pooled data from independent experiments are shown in Fig. 5.

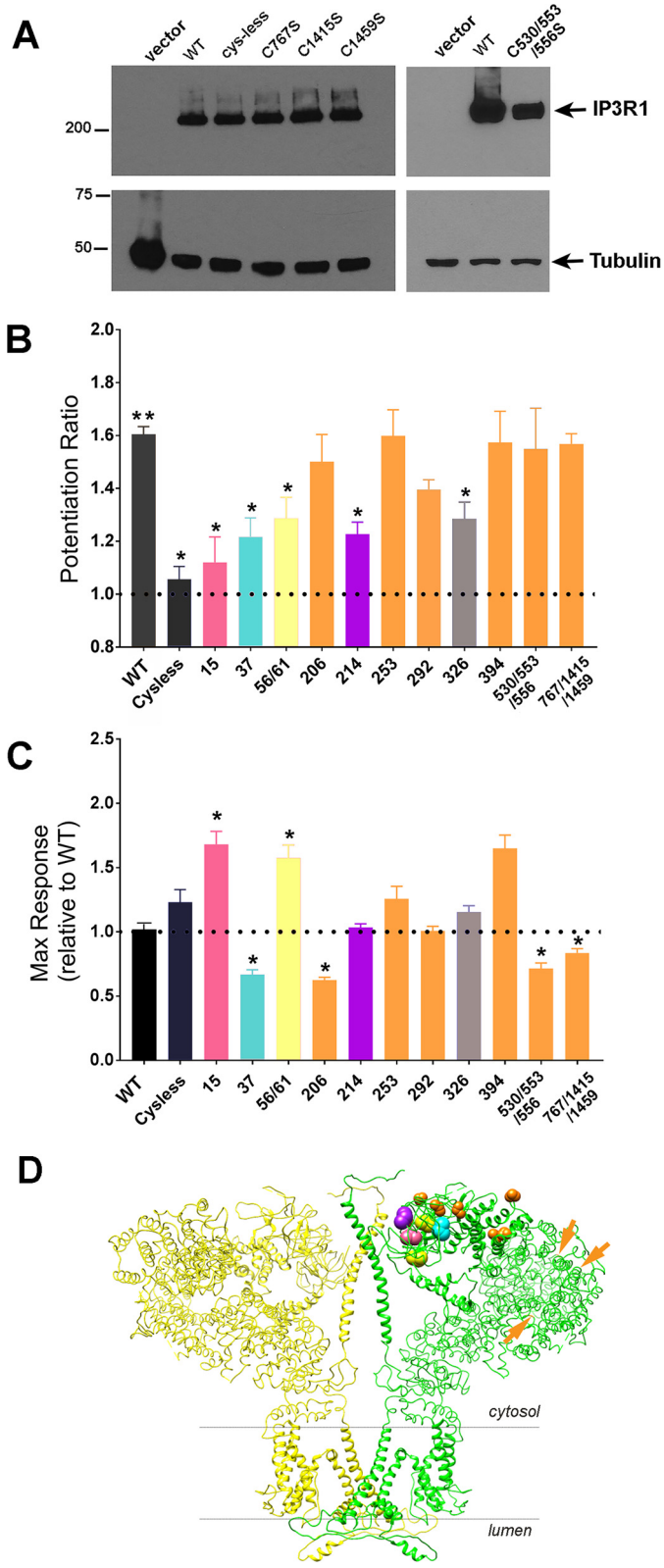


**Figure 5. Quantitation of thimerosal potentiation of carbachol-mediated intracellular $Ca^{2+}$ release for specific cysteine mutants of $IP_3R1$.** *A*, expression of selected cysteine mutants in 3KO cells detected by immunoblotting with $IP_3R1$ Ab. The expression of the remaining cysteine mutants used in this study has been verified previously (33). *B*, the amplitude of the $Ca^{2+}$ response to 0.25 $\mu$M carbachol after thimerosal treatment was expressed as a ratio to the control response using data obtained as shown in Fig. 4*E*. *C*, the response to a maximal dose of carbachol (20 $\mu$M) was quantitated for each mutant and expressed as a ratio of WT $IP_3R1$ responses. All data are the means ± S.E. of $n = 3–6$ independent experiments. *, $p < 0.001$ significantly different from WT; **, $p < 0.0001$ significantly different from 1 (one sample *t* test). *D*, two opposing subunits of the tetrameric structure of apo-$IP_3R1$ determined by cryo-EM (Protein Data Bank (PDB) ID 3JAV) are shown in a side view. The redox-sensitive cysteine residues are color coded according to the data in *B*. Redox-insensitive residues are colored *orange*. Side chains for Cys-767, Cys-1415, and Cys-1459 were not resolved in the structure and are indicated by *orange arrows*. Cys-326, which is located in the SI splice site, was also not present in the structure.

the $IP_3R$ would be predominantly oxidized. However, it is now understood that conditions favoring oxidative protein folding can occur under more reducing conditions and that the reactive thiols of key ER luminal oxidoreductases are predominantly in the reduced state (47–49). Indeed, under basal conditions only Cys-2496 and Cys-2533 of the five intraluminal $IP_3R1$ cysteines were found to be oxidized. The pair of intraluminal cysteines at Cys-2496 and Cys-2504 have previously been suggested to form a disulfide bond based on NMR studies of a fusion protein encoding the intraluminal loop (50). However, in our experiments Cys-2504 was consistently reduced, and therefore a disulfide bond between these residues is unlikely to occur in an intact cell under basal conditions. Both Cys-2496 and Cys-2504 have been implicated as important for association with ERp44, an intraluminal chaperone of the thioredoxin family, which selectively associates with the reduced form of $IP_3R1$ and has an inhibitory effect on channel function (51). Our results would suggest that ERp44 would preferentially associate with the Cys-2504 residue under basal conditions. The Cys-2533 residue is located at the intraluminal end of a pore helix, and mutation of this residue has previously been shown to inactivate channel function (52). A constitutively oxidized Cys-2533 residue may stabilize the intraluminal structure of the pore, possibly by formation of disulfide bonds with other ER luminal proteins. Neither thimerosal nor $H_2O_2$ changed the redox state of $IP_3R$ intraluminal thiols.

Despite the reducing environment in the cytosol, a significant number of cysteines in key cytosolic signaling proteins are in the oxidized state (53). In the case of $IP_3R1$, two cytosol-facing cysteines (Cys-292 and Cys-1415) were found to be oxidized under basal conditions. This could indicate that these thiols have a sufficiently low p$K_a$ to allow the formation of thiolate anions that can form disulfides with GSH or with other redox-sensitive proteins. It is also possible that $IP_3Rs$ are present in a local environment that is more oxidizing than the bulk redox potential of the cytosol (54).

Mass spectroscopy indicated a total of 11 cytosolic cysteines that were modified in the presence of thimerosal. However, there was considerable variability in the results with some of the cysteines being modified in only one of three experiments. The reason for this variability is not clear but could be related to the experimental methodology and/or heterogeneity in the redox state of specific cysteines in the $IP_3R$. Only three cysteines were consistently oxidized by thimerosal in all three experiments, and they were Cys-206, Cys-767, and Cys-1459. In the case of $H_2O_2$, there were also three cysteines that were oxidized in each of two experiments. They were Cys-206, Cys-214, and Cys-1397. Cys-206 and Cys-214 are located in the SD, whereas Cys-767, Cys-1397, and Cys-1459 are located in the regulatory domain. To assess the functional relevance of these

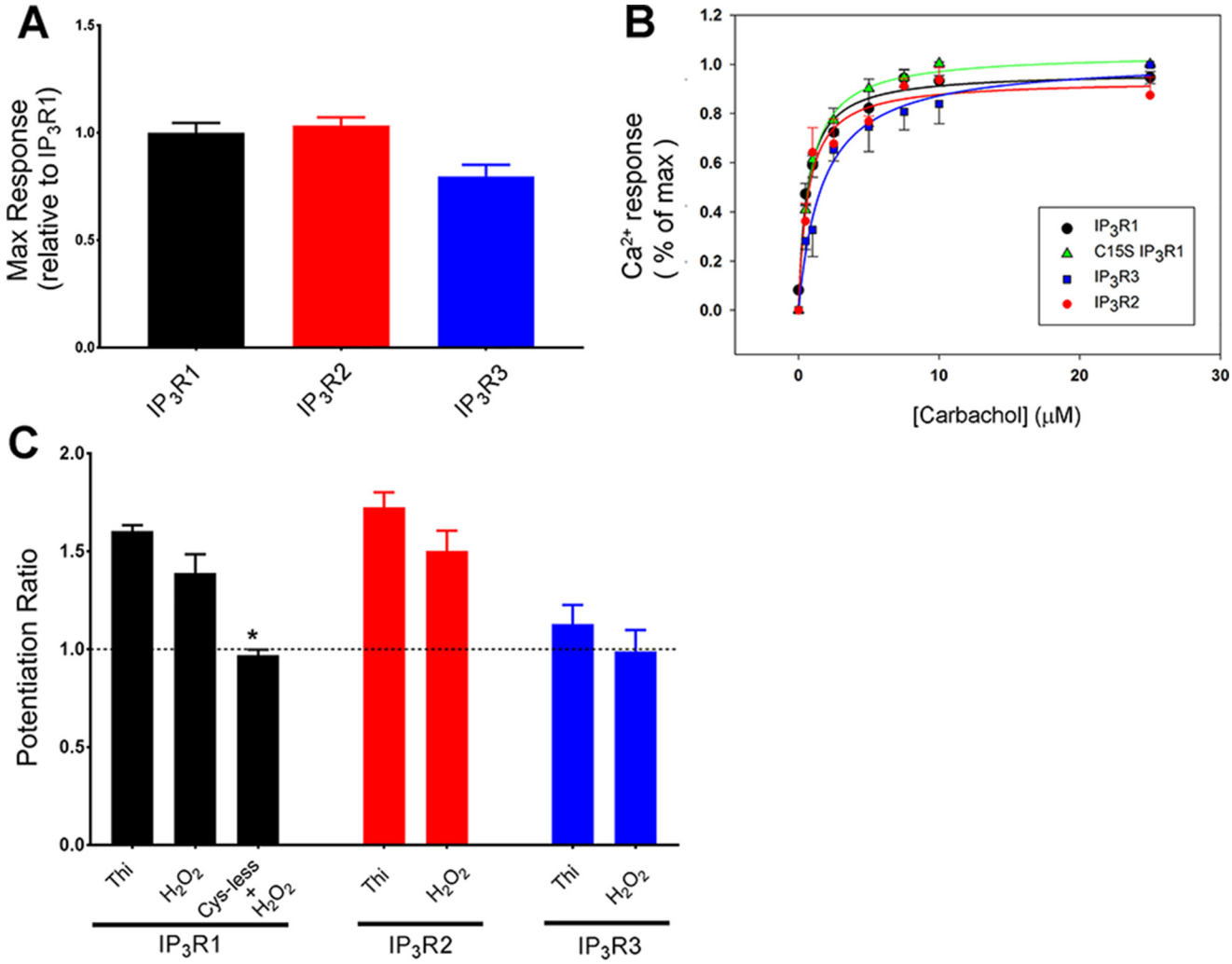


**Figure 6. Redox potentiation by thimerosal and $H_2O_2$ of $IP_3R1$, $IP_3R2$, and $IP_3R3$.** *A*, the three different $IP_3R$ isoforms were transfected into HEK293 3KO cells (10 $\mu$g of DNA/60-cm plate) and the maximal $Ca^{2+}$ response obtained with 25 $\mu$M carbachol in each experiment was quantitated relative to the maximal response for $IP_3R1$. *B*, intracellular $Ca^{2+}$ release was measured using different concentrations of carbachol. Also shown are the responses of the C15S $IP_3R1$ mutant. The amplitude of the $Ca^{2+}$ response was normalized to the maximum and is shown as means ± S.E. ($n = 3$). The *lines* drawn through the data points are fits to the equation $y = ax/(b + x)$, where $b$ corresponds to the $EC_{50}$ values (given in the text). *C*, the 3KO cells transfected with the three different isoforms were pretreated for 2 min with either 10 $\mu$M thimerosal (*Thi*) or 100 $\mu$M $H_2O_2$, and the potentiation of responses to 0.25 $\mu$M carbachol or 0.5 $\mu$M carbachol ($IP_3R3$) was measured as described in Fig. 5*B*. The data shown are means ± S.E. of three to five independent experiments. *, $p < 0.05$ statistical significant from thimerosal for each isoform.

residues, we have used an assay in which cysteine mutants were transfected into HEK293 $IP_3R$ 3KO cells. Redox potentiation was measured by preincubating cells for 2 min with oxidant prior to stimulation of intracellular $Ca^{2+}$ mobilization with a subsaturating concentration of carbachol. These studies revealed that redox sensitivity was lost in an $IP_3R1$ mutant lacking the N-terminal 12 cysteines. Further mutagenesis of the individual cysteines indicates that multiple cysteines confer redox sensitivity to thimerosal. With the exception of Cys-326, all the redox-sensitive residues are clustered in the SD (Fig. 5*D*).

The SD (also referred to as the $\beta$-trefoil domain 1 (34)) plays a critical role in channel gating (35–37). This domain makes contacts with two adjacent downstream domains called the $\beta$-trefoil domain-2 and the armadillo solenoid fold-1 domain, which together constitute the inner binding core that specifically binds $IP_3$ (30). The cryo-EM structures of apo-$IP_3R1$ (34) and multiple liganded form of $IP_3R3$ (55) have been reported. Long-range conformational changes resulting from $IP_3$ binding can be transmitted to the channel domain by several mechanisms (34, 55). This includes changes in the relative position of a loop variously referred to as a "hot spot" or "gating loop" within the SD that contains the Tyr-167 residue. Mutations within the Tyr-167 loop disrupt the coupling between $IP_3$ binding and channel opening (56). We suggest that the oxidation of specific cysteines in the SD may enhance the coupling efficiency of the mechanisms by which the SD transduces the ligand-binding signal to the channel domain. This is consistent with earlier studies that found an interaction between recombinant SD and inner binding core proteins that was strengthened by adding thimerosal (32). A more detailed understanding of the molecular mechanism of redox potentiation of the $IP_3R$ channel awaits high resolution structures of the open state of the $IP_3R1$ channel. Oxidation of key thiols could also influence channel activity indirectly by modifying interactions of the receptor with its many binding partners. For example, one of the interaction sites of Bcl-2 encompasses the $H_2O_2$-sensitive

Cys-1397 (57). Interestingly, an R36C mutation within the SD has been identified in three affected individuals with spinocerebellar ataxia (58). This mutation would place a cysteine immediately adjacent to the redox-sensitive Cys-37 residue. Unlike other inactivating $IP_3R1$ mutations linked to inherited neurodegenerative diseases, this mutation results in a gain of channel function. The redox regulation properties of the R36C mutant remain to be investigated.

An additional finding in the present study was that the results from MS and functional assays were not always well-correlated. For example, several residues were reproducibly oxidized by thimerosal in the MS measurements but played no role when tested in functional assays (*e.g.* Cys-206, Cys-767, Cys-1415, and Cys-1459). Cys-206 has previously been shown to be a highly accessible cysteine (33) and was oxidized by both thimerosal and $H_2O_2$. However, robust oxidation of specific thiols may simply reflect their higher accessibility/reactivity and may not necessarily result in altered channel function. There were also several cysteine residues that contributed to redox potentiation in functional measurements that were not detected as being oxidized in the MS assay (*e.g.* Cys-15 and Cys-326). A functional effect obtained from mutating a particular cysteine residue does not prove that this residue is the physiological target of oxidants in the WT receptor. Although there may be limitations regarding sensitivity and coverage, the MS analysis does accurately identify the redox-sensitive thiols of the $IP_3R$ *in situ*.

Although this study focused primarily on $IP_3R1$, we have also made some functional measurements on $IP_3R2$ and $IP_3R3$ expressed in HEK293 3KO cells. In line with previous studies on DT40 cells (31, 32), we observed reduced potentiation of $IP_3R3$ by thimerosal and $H_2O_2$ relative to $IP_3R1$ or $IP_3R2$ (Fig. 6). Five of the six cysteines present in the SD of $IP_3R1$ are highly conserved in all three isoforms; only Cys-15 is unique to $IP_3R1$, and its mutation markedly reduces redox potentiation of the $IP_3R1$ channel by either $H_2O_2$ or thimerosal. Although the remaining five cysteines are conserved, it is also apparent from $IP_3$-binding studies with chimeric receptors that the SD of $IP_3R3$ is unique and is not interchangeable with the other two isoforms (35, 59). Thus differences in the precise intra- and intermolecular contacts made by the SD may determine differences in redox regulation of the three isoforms. We also cannot exclude the possibility that other nonconserved cysteine residues outside of the SD may play a role in redox regulation of $IP_3R2$ and $IP_3R3$. Clearly other cell and species–specific regulatory factors can also play a role because previous studies on DT40 cells have noted that the endogenous chicken $IP_3R3$ and stably expressed rat $IP_3R3$ differ in their redox sensitivity (13). Different redox microenvironments (54) or variable antioxidant defenses could also contribute to differential sensitivity of $IP_3R$ isoforms in different cell types.

Redox regulation of $IP_3R$-mediated $Ca^{2+}$ signaling has been implicated in ER stress and apoptosis (19, 60–63). The redox-insensitive mutants identified in this study may be potentially useful in examining the contribution of $IP_3R$ redox regulation in different models of cellular injury.

## Materials and methods

### *Gel-shift assays for measurements of $IP_3R$ redox state*

The method used was a modification of the procedure described by Leichert and Jacob (20, 21). The key step is the quenching of the cellular redox state by rapid acidification of the cells with 10% TCA (Fig. 1*A*). The cells were scraped from the plates and centrifuged. The protein precipitate was dissolved in a strongly denaturing buffer (DB) containing 200 mM Tris-HCl (pH 8.5), 10 mM EDTA, 0.5% SDS, and 6 M urea. The lysate was incubated in this buffer supplemented with 10 mM iodoacetamide for 45 min to block all available free thiols. The lysate was then reprecipitated with 10% TCA and resuspended in DB buffer containing 10 mM DTT and incubated for a further 45 min. After reprecipitation with 10% TCA, the pellet was resuspended in 0.25 ml of DB buffer and adjusted to pH 7.0 with NaOH. Lysate protein (15 $\mu$g) was incubated with 0.5 mM PEG-maleimides of various sizes (2, 5, and 20 kDa) for 1 h. After SDS–PAGE on 5% gels for 2.5 h, the samples were transferred to nitrocellulose and immunoblotted with a C-terminal Ab specific for $IP_3R1$ raised to the C-terminal 18 amino acids (64). The size of the MPEG-shifted bands was estimated by comparing the relative mobility of the bands to standards retained on the 5% gels including the unmodified $IP_3R1$ subunit (320 kDa), a lysate from a stable HEK293 cell expressing a concatenated dimer of $IP_3R1$ (640 kDa) (65), prestained myosin (211 kDa), and prestained $\beta$-gal (114 kDa).

### *GSH assays*

Total GSH was measured in the supernatant of TCA-quenched cell lysates using an enzymatic recycling assay utilizing 5,5′-dithiobis(nitrobenzoic acid), NADPH, and GSH reductase as originally described (66). Oxidized GSH was measured with a lumiglo kit obtained from Promega (Madison, WI). HEK293 cells ($5 \times 10^4$) were grown for 24 h in 96-well plates and treated with various oxidants. The cells were lysed on the plate using a supplied buffer containing NEM to block GSH. Residual GSSG was converted to GSH and measured using a luciferin probe as described by the manufacturer.

### *Mass spectroscopy*

HEK293 cells were transfected with plasmid encoding rat $IP_3R1$ for 48 h. The cells were treated in the presence or absence of 50 $\mu$M thimerosal for 10 min. For each condition two 150-mm plates were used. After removal of the medium, each plate was quenched in 2.5 ml of 10% TCA. The precipitated protein was sequentially treated with iodoacetamide and DTT as described above for the gel-shift assays. The final DTT-treated lysate was solubilized in DB buffer and adjusted to a pH of 7.0. The lysate (1 mg of protein) was incubated with 0.5 mM biotin–maleimide (Sigma) for 16 h at room temperature in the dark. The reaction was terminated with 10 mM DTT, and the entire reaction was loaded on a PD-10 desalting column (GE Healthcare) equilibrated in a buffer containing 150 mM NaCl, 20 mM NaMOPS (pH 7.0), 0.5 mM EDTA, 0.2 mM DTT, 0.1% deoxycholate, and 0.2% Triton X-100. This buffer exchange step was carried out to reduce the SDS and urea concentrations to allow more efficient immunoprecipitation. The eluted pro-

tein was incubated with Ab to the C terminus of $IP_3R1$ and protein A–Sepharose overnight. Immunocomplexes were processed on 5% SDS–PAGE and stained with silver (SilverSNAP stain; Thermo Fisher Scientific) or with colloidal blue (Novex). The excised band above the myosin marker was processed for in-gel trypsin digestion and LC—MS/MS using a Thermo Q Exactive Plus mass spectrometer at the Wistar Proteomics facility (Wistar Institute, Philadelphia, PA). Peptide identification was achieved by searching against the rat $IP_3R1$ (NP_001007236.2) and the nonredundant human database from the National Center for Biotechnology Information. Mass accuracy was limited to 10 ppm for precursor ions and 0.6 Da for product ions, with tryptic enzyme specificity and up to two missed cleavages. Variable modifications included cysteine alkylation by iodoacetamide (+57.02 Da) and reaction with biotin–maleimide (+451.54 Da) (67).

### Cytosolic [$Ca^{2+}$] measurement in HEK293 cells

The cells were grown in 60-cm plates to ~70% confluence and were transfected with 10 $\mu$g of $IP_3R$ DNA using Lipofectamine 3000 according to the manufacturer's instructions (Thermo Fisher Scientific). After 24 h, the cells were removed with trypsin and seeded at 50,000 cells/well in a 96-well transparent black plate. The culture medium was removed after a further 24 h and replaced with 90 $\mu$l of Hanks' buffered salt solution, 10 mM HEPES (pH 7.2) (HBSS–HEPES) for 30 min. An additional 100 $\mu$l of HBSS–HEPES containing 5 $\mu$M Fluo-8 AM, 0.1 mM sulfinpyrazone, and 500 $\mu$M Brilliant Black (to quench extracellular dye fluorescence) was added to the plates, which were incubated for 1 h at 37 °C. Changes in cytosolic $Ca^{2+}$ were monitored using a Flex Station II plate reader in the fluorescence mode. The plate was maintained at 37 °C, and measurements were made using excitation and emission wavelengths of 485 and 525 nm, respectively. The various additions of thimerosal, $H_2O_2$, and carbachol were made utilizing the fluidics addition system of the Flex station II. Data acquisition and analysis was carried out with SoftMax Pro and Excel.

### DNA constructs and cysteine mutagenesis

The cDNA encoding the $IP_3R1$ isoform was a gift of Dr. Greg Mignery (Loyola University, Chicago, IL) and encoded the splice variant SI(+), SII(+), SIII(−). All amino acid numbering is with reference to the rat $IP_3R1$ (68). The cDNA encoding mouse $IP_3R2$ was a gift of Dr. Katsuhiko Mikoshiba (69), and rat $IP_3R3$ was a gift of Dr. Graeme Bell (70). The Cys-less construct was a kind gift of Dr. Colin Taylor and contains mutations of the first 12 N-terminal cysteines modified to alanine in $IP_3R1$ (SI(−)). The Cys-less construct has previously been shown to retain channel function (30, 31). Individual mutation of each of the 12 N-terminal cysteines to serine was described previously and included an additional cysteine located within the SI splice site (C326S) (33). The C530A/C553A/C556A mutant was produced by excising the BamHI/KpnI fragment from the Cys-less mutant and replacing it with the BamHI/KpnI PCR-amplified product derived from WT $IP_3R1$. The three amino acids Cys-767, Cys-1415, and Cys-1459 were changed to serine using the QuikChange II XL site-directed mutagenesis kit (Agilent Technologies; catalog no. 200521) and the primer design method developed by Zheng *et al.* (71).

### Antibodies and reagents

MPEG-2 and MPEG-20 was purchased from Nektar (Huntsville, AL). MPEG-5, sulfinpyrazone, and Brilliant Black were obtained from Sigma. Fluo-8AM was from AbCam (Cambridge, MA).

*Author contributions*—S. K. J. conceptualization; S. K. J. funding acquisition; S. K. J. writing-original draft; S. K. J. project administration; S. K. J. writing-review and editing; M. Y., D. I. Y., M. A., D. M. B., and G. H. investigation; K. A. methodology.

*Acknowledgment—We thank Colin Taylor for the Cys-less mutant.*

### References


1. Elferink, J. G. (1999) Thimerosal: a versatile sulfhydryl reagent, calcium mobilizer, and cell function-modulating agent. *Gen. Pharmacol.* **33,** 1–6 CrossRef Medline
2. Bird, G. S., Burgess, G. M., and Putney, J. W., Jr. (1993) Sulfhydryl reagents and cAMP-dependent kinase increase the sensitivity of the inositol 1,4,5-trisphosphate receptor in hepatocytes. *J. Biol. Chem.* **268,** 17917–17923 Medline
3. Pruijn, F. B., Sibeijn, J. P., and Bast, A. (1990) Changes in inositol-1,4,5-trisphosphate binding to hepatic plasma membranes caused by temperature, *N*-ethylmaleimide and menadione. *Biochem. Pharmacol.* **40,** 1947–1952 CrossRef Medline
4. Redondo, P. C., Salido, G. M., Rosado, J. A., and Pariente, J. A. (2004) Effect of hydrogen peroxide on $Ca^{2+}$ mobilisation in human platelets through sulphydryl oxidation dependent and independent mechanisms. *Biochem. Pharmacol.* **67,** 491–502 CrossRef Medline
5. Islam, M. S., Kindmark, H., Larsson, O., and Berggren, P. O. (1997) Thiol oxidation by 2,2′-dithiodipyridine causes a reversible increase in cytoplasmic free $Ca^{2+}$ concentration in pancreatic beta-cells: role for inositol 1,4,5-trisphosphate-sensitive $Ca^{2+}$ stores. *Biochem. J.* **321,** 347–354 CrossRef Medline
6. Lock, J. T., Sinkins, W. G., and Schilling, W. P. (2011) Effect of protein *S*-glutathionylation on $Ca^{2+}$ homeostasis in cultured aortic endothelial cells. *Am. J. Physiol. Heart Circ. Physiol.* **300,** H493–H506 CrossRef Medline
7. Lock, J. T., Sinkins, W. G., and Schilling, W. P. (2012) Protein *S*-glutathionylation enhances $Ca^{2+}$-induced $Ca^{2+}$ release via the $IP_3$ receptor in cultured aortic endothelial cells. *J. Physiol.* **590,** 3431–3447 CrossRef Medline
8. Henschke, P. N., and Elliott, S. J. (1995) Oxidized glutathione decreases luminal $Ca^{2+}$ content of the endothelial cell Ins(1,4,5)P3-sensitive $Ca^{2+}$ store. *Biochem. J.* **312,** 485–489 CrossRef Medline
9. Renard, D. C., Seitz, M. B., and Thomas, A. P. (1992) Oxidized glutathione causes sensitization of calcium release to inositol 1,4,5-trisphosphate in permeabilized hepatocytes. *Biochem. J.* **284,** 507–512 CrossRef Medline
10. Madesh, M., Hawkins, B. J., Milovanova, T., Bhanumathy, C. D., Joseph, S. K., Ramachandrarao, S. P., Sharma, K., Kurosaki, T., and Fisher, A. B. (2005) Selective role for superoxide in $InsP_3$ receptor-mediated mitochondrial dysfunction and endothelial apoptosis. *J. Cell Biol.* **170,** 1079–1090 CrossRef Medline
11. Suzuki, Y. J., and Ford, G. D. (1992) Superoxide stimulates $IP_3$-induced $Ca^{2+}$ release from vascular smooth muscle sarcoplasmic reticulum. *Am. J. Physiol.* **262,** H114–H116 Medline
12. Wesson, D. E., and Elliott, S. J. (1995) The $H_2O_2$-generating enzyme, xanthine oxidase, decreases luminal $Ca^{2+}$ content of the $IP_3$-sensitive $Ca^{2+}$ store in vascular endothelial cells. *Microcirculation* **2,** 195–203 CrossRef Medline
13. Bansaghi, S., Golenár, T., Madesh, M., Csordás, G., RamachandraRao, S., Sharma, K., Yule, D. I., Joseph, S. K., and Hajnóczky, G. (2014) Isoform- and species-specific control of inositol 1,4,5-trisphosphate ($IP_3$) receptors

by reactive oxygen species. *J. Biol. Chem.* **289,** 8170–8181 CrossRef Medline
14. Kaplin, A. I., Ferris, C. D., Voglmaier, S. M., and Snyder, S. H. (1994) Purified reconstituted inositol 1,4,5-trisphosphate receptors: thiol reagents act directly on receptor protein. *J. Biol. Chem.* **269,** 28972–28978 Medline
15. Thrower, E. C., Duclohier, H., Lea, E. J., Molle, G., and Dawson, A. P. (1996) The inositol 1,4,5-trisphosphate-gated $Ca^{2+}$ channel: effect of the protein thiol reagent thimerosal on channel activity. *Biochem. J.* **318,** 61–66 CrossRef Medline
16. Vais, H., Siebert, A. P., Ma, Z., Fernández-Mongil, M., Foskett, J. K., and Mak, D. O. (2010) Redox-regulated heterogeneous thresholds for ligand recruitment among $InsP_3R$ $Ca^{2+}$-release channels. *Biophys. J.* **99,** 407–416 CrossRef Medline
17. Li, G., Mongillo, M., Chin, K. T., Harding, H., Ron, D., Marks, A. R., and Tabas, I. (2009) Role of ERO1-$\alpha$-mediated stimulation of inositol 1,4,5-triphosphate receptor activity in endoplasmic reticulum stress-induced apoptosis. *J. Cell Biol.* **186,** 783–792 CrossRef Medline
18. Anelli, T., Bergamelli, L., Margittai, E., Rimessi, A., Fagioli, C., Malgaroli, A., Pinton, P., Ripamonti, M., Rizzuto, R., and Sitia, R. (2012) Ero1$\alpha$ regulates $Ca^{2+}$ fluxes at the endoplasmic reticulum-mitochondria interface (MAM). *Antioxid. Redox Signal.* **16,** 1077–1087 CrossRef Medline
19. Kiviluoto, S., Vervliet, T., Ivanova, H., Decuypere, J. P., De Smedt, H., Missiaen, L., Bultynck, G., and Parys, J. B. (2013) Regulation of inositol 1,4,5-trisphosphate receptors during endoplasmic reticulum stress. *Biochim. Biophys. Acta* **1833,** 1612–1624 CrossRef Medline
20. Leichert, L. I., and Jakob, U. (2004) Protein thiol modifications visualized *in vivo*. *PLoS Biol.* **2,** e333 CrossRef Medline
21. Leichert, L. I., and Jakob, U. (2006) Global methods to monitor the thiol-disulfide state of proteins *in vivo*. *Antioxid. Redox Signal.* **8,** 763–772 CrossRef Medline
22. Wojcikiewicz, R. J. (1995) Type I, II, and III inositol 1,4,5-trisphosphate receptors are unequally susceptible to down-regulation and are expressed in markedly different proportions in different cell types. *J. Biol. Chem.* **270,** 11678–11683 CrossRef Medline
23. Makmura, L., Hamann, M., Areopagita, A., Furuta, S., Muñoz, A., and Momand, J. (2001) Development of a sensitive assay to detect reversibly oxidized protein cysteine sulfhydryl groups. *Antioxid. Redox Signal.* **3,** 1105–1118 CrossRef Medline
24. Schwaller, M., Wilkinson, B., and Gilbert, H. F. (2003) Reduction-reoxidation cycles contribute to catalysis of disulfide isomerization by protein-disulfide isomerase. *J. Biol. Chem.* **278,** 7154–7159 CrossRef Medline
25. Renard-Rooney, D. C., Joseph, S. K., Seitz, M. B., and Thomas, A. P. (1995) Effect of oxidized glutathione and temperature on inositol 1,4,5-trisphosphate binding in permeabilized hepatocytes. *Biochem. J.* **310,** 185–192 CrossRef Medline
26. James, S. J., Slikker, W., 3rd, Melnyk, S., New, E., Pogribna, M., and Jernigan, S. (2005) Thimerosal neurotoxicity is associated with glutathione depletion: protection with glutathione precursors. *Neurotoxicology* **26,** 1–8 CrossRef Medline
27. Kosower, N. S., Kosower, E. M., Wertheim, B., and Correa, W. S. (1969) Diamide, a new reagent for the intracellular oxidation of glutathione to the disulfide. *Biochem. Biophys. Res. Commun.* **37,** 593–596 CrossRef Medline
28. Alzayady, K. J., Wang, L., Chandrasekhar, R., Wagner, L. E., 2nd, Van Petegem, F., and Yule, D. I. (2016) Defining the stoichiometry of inositol 1,4,5-trisphosphate binding required to initiate $Ca^{2+}$ release. *Sci. Signal.* **9,** ra35 CrossRef Medline
29. Mataragka, S., and Taylor, C. W. (2018) All three $IP_3$ receptor subtypes generate $Ca^{2+}$ puffs, the universal building blocks of IP3-evoked $Ca^{2+}$ signals. *J. Cell Sci.* **131,** jcs220848 CrossRef Medline
30. Seo, M. D., Velamakanni, S., Ishiyama, N., Stathopulos, P. B., Rossi, A. M., Khan, S. A., Dale, P., Li, C., Ames, J. B., Ikura, M., and Taylor, C. W. (2012) Structural and functional conservation of key domains in $InsP_3$ and ryanodine receptors. *Nature* **483,** 108–112 CrossRef Medline
31. Khan, S. A., Rossi, A. M., Riley, A. M., Potter, B. V., and Taylor, C. W. (2013) Subtype-selective regulation of $IP_3$ receptors by thimerosal via cysteine residues within the $IP_3$-binding core and suppressor domain. *Biochem. J.* **451,** 177–184 CrossRef Medline
32. Bultynck, G., Szlufcik, K., Kasri, N. N., Assefa, Z., Callewaert, G., Missiaen, L., Parys, J. B., and De Smedt, H. (2004) Thimerosal stimulates $Ca^{2+}$ flux through inositol 1,4,5-trisphosphate receptor type 1, but not type 3, via modulation of an isoform-specific $Ca^{2+}$-dependent intramolecular interaction. *Biochem. J.* **381,** 87–96 CrossRef Medline
33. Joseph, S. K., Nakao, S. K., and Sukumvanich, S. (2006) Reactivity of free thiol groups in type-I inositol trisphosphate receptors. *Biochem. J.* **393,** 575–582 CrossRef Medline
34. Fan, G., Baker, M. L., Wang, Z., Baker, M. R., Sinyagovskiy, P. A., Chiu, W., Ludtke, S. J., and Serysheva, I. I. (2015) Gating machinery of $InsP_3R$ channels revealed by electron cryomicroscopy. *Nature* **527,** 336–341 CrossRef Medline
35. Iwai, M., Michikawa, T., Bosanac, I., Ikura, M., and Mikoshiba, K. (2007) Molecular basis of the isoform-specific ligand-binding affinity of inositol 1,4,5-trisphosphate receptors. *J. Biol. Chem.* **282,** 12755–12764 CrossRef Medline
36. Rossi, A. M., Riley, A. M., Tovey, S. C., Rahman, T., Dellis, O., Taylor, E. J., Veresov, V. G., Potter, B. V., and Taylor, C. W. (2009) Synthetic partial agonists reveal key steps in $IP_3$ receptor activation. *Nat. Chem. Biol.* **5,** 631–639 CrossRef Medline
37. Chan, J., Yamazaki, H., Ishiyama, N., Seo, M. D., Mal, T. K., Michikawa, T., Mikoshiba, K., and Ikura, M. (2010) Structural studies of inositol 1,4,5-trisphosphate receptor: coupling ligand binding to channel gating. *J. Biol. Chem.* **285,** 36092–36099 CrossRef Medline
38. Miyakawa, T., Maeda, A., Yamazawa, T., Hirose, K., Kurosaki, T., and Iino, M. (1999) Encoding of calcium signals by differential expression of $IP_3$ receptor subtypes. *EMBO J.* **18,** 1303–1308 CrossRef Medline
39. Chandrasekhar, R., Alzayady, K. J., Wagner, L. E., 2nd, and Yule, D. I. (2016) Unique regulatory properties of heterotetrameric inositol 1,4,5-trisphosphate receptors revealed by studying concatenated receptor constructs. *J. Biol. Chem.* **291,** 4846–4860 CrossRef Medline
40. Dutta, A., Tirupula, K. C., Alexiev, U., and Klein-Seetharaman, J. (2010) Characterization of membrane protein non-native states: 1. Extent of unfolding and aggregation of rhodopsin in the presence of chemical denaturants. *Biochemistry* **49,** 6317–6328 CrossRef Medline
41. Borgnia, M. J., Kozono, D., Calamita, G., Maloney, P. C., and Agre, P. (1999) Functional reconstitution and characterization of AqpZ, the *E. coli* water channel protein. *J. Mol. Biol.* **291,** 1169–1179 CrossRef Medline
42. Heinz, C., Engelhardt, H., and Niederweis, M. (2003) The core of the tetrameric mycobacterial porin MspA is an extremely stable $\beta$-sheet domain. *J. Biol. Chem.* **278,** 8678–8685 CrossRef Medline
43. Chaube, R., Hess, D. T., Wang, Y. J., Plummer, B., Sun, Q. A., Laurita, K., and Stamler, J. S. (2014) Regulation of the skeletal muscle ryanodine receptor/$Ca^{2+}$-release channel RyR1 by *S*-palmitoylation. *J. Biol. Chem.* **289,** 8612–8619 CrossRef Medline
44. Fredericks, G. J., Hoffmann, F. W., Rose, A. H., Osterheld, H. J., Hess, F. M., Mercier, F., and Hoffmann, P. R. (2014) Stable expression and function of the inositol 1,4,5-triphosphate receptor requires palmitoylation by a DHHC6/selenoprotein K complex. *Proc. Natl. Acad. Sci. U.S.A.* **111,** 16478–16483 CrossRef Medline
45. Ji, Y., Leymarie, N., Haeussler, D. J., Bachschmid, M. M., Costello, C. E., and Lin, C. (2013) Direct detection of *S*-palmitoylation by mass spectrometry. *Anal Chem* **85,** 11952–11959 CrossRef Medline
46. Hwang, C., Sinskey, A. J., and Lodish, H. F. (1992) Oxidized redox state of glutathione in the endoplasmic reticulum. *Science* **257,** 1496–1502 CrossRef Medline
47. Chakravarthi, S., Jessop, C. E., and Bulleid, N. J. (2006) The role of glutathione in disulphide bond formation and endoplasmic-reticulum-generated oxidative stress. *EMBO Reports* **7,** 271–275 CrossRef Medline
48. Appenzeller-Herzog, C. (2011) Glutathione- and non-glutathione-based oxidant control in the endoplasmic reticulum. *J. Cell Sci.* **124,** 847–855 CrossRef Medline
49. Hudson, D. A., Gannon, S. A., and Thorpe, C. (2015) Oxidative protein folding: from thiol-disulfide exchange reactions to the redox poise of the endoplasmic reticulum. *Free Radic. Biol. Med.* **80,** 171–182 CrossRef Medline
50. Kang, S., Kang, J., Kwon, H., Frueh, D., Yoo, S. H., Wagner, G., and Park, S. (2008) Effects of redox potential and $Ca^{2+}$ on Inositol 1,4,5-trisphosphate

receptor L3–1 loop region: implications for receptor regulation. *J. Biol. Chem.* **283,** 25567–25575 CrossRef Medline

51. Higo, T., Hattori, M., Nakamura, T., Natsume, T., Michikawa, T., and Mikoshiba, K. (2005) Subtype-specific and ER lumenal environment-dependent regulation of inositol 1,4,5-trisphosphate receptor type 1 by ERp44. *Cell* **120,** 85–98 CrossRef Medline
52. Schug, Z. T., da Fonseca, P. C., Bhanumathy, C. D., Wagner, L., 2nd, Zhang, X., Bailey, B., Morris, E. P., Yule, D. I., and Joseph, S. K. (2008) Molecular characterization of the inositol 1,4,5-trisphosphate pore-forming segment. *J. Biol. Chem.* **283,** 2939–2948 CrossRef Medline
53. Go, Y. M., Duong, D. M., Peng, J., and Jones, D. P. (2011) Protein cysteines map to functional networks according to steady-state level of oxidation. *J. Proteomics Bioinform.* **4,** 196–209 Medline
54. Booth, D. M., Enyedi, B., Geiszt, M., Várnai, P., and Hajnóczky, G. (2016) Redox nanodomains are induced by and control calcium signaling at the ER–mitochondrial interface. *Mol. Cell* **63,** 240–248 CrossRef Medline
55. Paknejad, N., and Hite, R. K. (2018) Structural basis for the regulation of inositol trisphosphate receptors by $Ca^{2+}$ and $IP_3$. *Nat. Struct. Mol. Biol.* **25,** 660–668 CrossRef Medline
56. Yamazaki, H., Chan, J., Ikura, M., Michikawa, T., and Mikoshiba, K. (2010) Tyr-167/Trp-168 in type1/3 inositol 1,4,5-trisphosphate receptor mediates functional coupling between ligand binding and channel opening. *J. Biol. Chem.* **285,** 36081–36091 CrossRef Medline
57. Rong, Y. P., Barr, P., Yee, V. C., and Distelhorst, C. W. (2009) Targeting Bcl-2 based on the interaction of its BH4 domain with the inositol 1,4,5-trisphosphate receptor. *Biochim. Biophys. Acta* **1793,** 971–978 CrossRef Medline
58. Casey, J. P., Hirouchi, T., Hisatsune, C., Lynch, B., Murphy, R., Dunne, A. M., Miyamoto, A., Ennis, S., van der Spek, N., O'Hici, B., Mikoshiba, K., and Lynch, S. A. (2017) A novel gain-of-function mutation in the ITPR1 suppressor domain causes spinocerebellar ataxia with altered $Ca^{2+}$ signal patterns. *J. Neurol.* **264,** 1444–1453 CrossRef Medline
59. Szlufcik, K., Bultynck, G., Callewaert, G., Missiaen, L., Parys, J. B., and De Smedt, H. (2006) The suppressor domain of inositol 1,4,5-trisphosphate receptor plays an essential role in the protection against apoptosis. *Cell Calcium* **39,** 325–336 CrossRef Medline
60. Back, S. H., and Kaufman, R. J. (2012) Endoplasmic reticulum stress and type 2 diabetes. *Annu. Rev. Biochem.* **81,** 767–793 CrossRef Medline
61. Simmen, T., Lynes, E. M., Gesson, K., and Thomas, G. (2010) Oxidative protein folding in the endoplasmic reticulum: tight links to the mitochondria-associated membrane (MAM). *Biochim. Biophys. Acta* **1798,** 1465–1473 CrossRef Medline
62. Mekahli, D., Bultynck, G., Parys, J. B., De Smedt, H., and Missiaen, L. (2011) Endoplasmic-reticulum calcium depletion and disease. *Cold Spring Harb. Perspect. Biol.* **3,** a004317 Medline
63. Ivanova, H., Vervliet, T., Missiaen, L., Parys, J. B., De Smedt, H., and Bultynck, G. (2014) Inositol 1,4,5-trisphosphate receptor-isoform diversity in cell death and survival. *Biochim. Biophys. Acta* **1843,** 2164–2183 CrossRef Medline
64. Joseph, S. K., and Samanta, S. (1993) Detergent solubility of the inositol trisphosphate receptor in rat brain membranes: evidence for association of the receptor with ankyrin. *J. Biol. Chem.* **268,** 6477–6486 Medline
65. Alzayady, K. J., Wagner, L. E., 2nd, Chandrasekhar, R., Monteagudo, A., Godiska, R., Tall, G. G., Joseph, S. K., and Yule, D. I. (2013) Functional inositol 1,4,5-trisphosphate receptors assembled from concatenated homo- and heteromeric subunits. *J. Biol. Chem.* **288,** 29772–29784 CrossRef Medline
66. Tietze, F. (1969) Enzymic method for quantitative determination of nanogram amounts of total and oxidized glutathione: applications to mammalian blood and other tissues. *Anal. Biochem.* **27,** 502–522 CrossRef Medline
67. Muthuramalingam, M., Matros, A., Scheibe, R., Mock, H. P., and Dietz, K. J. (2013) The hydrogen peroxide-sensitive proteome of the chloroplast *in vitro* and *in vivo*. *Front. Plant Sci.* **4,** 54 Medline
68. Mignery, G. A., Newton, C. L., Archer, B. T., 3rd, and Südhof, T. C. (1990) Structure and expression of the rat inositol 1,4,5-trisphosphate receptor. *J. Biol. Chem.* **265,** 12679–12685 Medline
69. Iwai, M., Tateishi, Y., Hattori, M., Mizutani, A., Nakamura, T., Futatsugi, A., Inoue, T., Furuichi, T., Michikawa, T., and Mikoshiba, K. (2005) Molecular cloning of mouse type 2 and type 3 inositol 1,4,5-trisphosphate receptors and identification of a novel type 2 receptor splice variant. *J. Biol. Chem.* **280,** 10305–10317 CrossRef Medline
70. Blondel, O., Takeda, J., Janssen, H., Seino, S., and Bell, G. (1993) Sequence and functional characterization of a third inositol trisphosphate receptor subtype, $IP_3R$-3, expressed in pancreatic islets, kidney, gastrointestinal tract, and other tissues. *J. Biol. Chem.* **268,** 11356–11363 Medline
71. Zheng, L., Baumann, U., and Reymond, J. L. (2004) An efficient one-step site-directed and site-saturation mutagenesis protocol. *Nucleic Acids Res.* **32,** e115 CrossRef Medline

# Redox regulation of type-I inositol trisphosphate receptors in intact mammalian cells

Suresh K. Joseph, Michael P. Young, Kamil Alzayady, David I. Yule, Mehboob Ali, David M. Booth and György Hajnóczky

*J. Biol. Chem. 2018, 293:17464-17476.*
*doi: 10.1074/jbc.RA118.005624 originally published online September 18, 2018*